Absolute differential cross sections for electron-impact excitation of CO near threshold: I. The valence states of CO

1996 J. Phys. B: At. Mol. Opt. Phys. 29 813

(http://iopscience.iop.org/0953-4075/29/4/021)

J. Phys. B: At. Mol. Opt. Phys. **29** (1996) 813–838. Printed in the UK

Absolute differential cross sections for electron-impact excitation of CO near threshold: I. The valence states of CO

J Zobel, U Mayer, K Jung and H Ehrhardt

Fachbereich Physik, Universitat Kaiserslautern, D-67663 Kaiserslautern, Germany

Received 18 August 1995, in final form 24 November 1995

Abstract. Absolute differential cross sections for the electronic excitation of valence states in CO have been measured in the energy range from threshold to 3.7 eV. In particular, a newly developed experimental technique to control the analyser's efficiency allowed us to measure absolute angular dependences of those states for scattering angles between 20° and 140°. The transitions from the X $^1\Sigma^+$ ground state to the a $^3\Pi$ and a′ $^3\Sigma^+$ states are forbidden by spin selection rules. It is found that the $^2\Pi$ shape resonance located at 1.8 eV partly decays into these valence states, which are located several eV above the resonance. The decay occurs by ejection of a core electron whose spin is antiparallel to that of the incident electron causing a sharp rise of the cross sections just at threshold. Three new core-excited shape resonances were found, one for each of $^2\Delta$, $^2\Sigma$ and $^2\Pi$ symmetry. By comparison with recently calculated cross sections their electron configurations have been classified. Resonant excitation via these three resonances or via the low-lying $^2\Pi$ resonance dominates the cross sections of the two spin forbidden transitions in the detected energy range. The excitation of the optically allowed X $^1\Sigma^+ \rightarrow$ A $^1\Pi$ transition, however, is dominated by non-resonant processes.

1. Introduction

In contrast to the electronic elastic rotational and vibrational excitation of molecules, the electronic excitation of molecules is, in general, accompanied by drastic changes of the molecular properties such as the dipole moment or the polarizability. The dipole moment can be an order of magnitude and the polarizability even three orders of magnitude higher than in the electronic ground state of the molecule. Consequently, the slow outgoing electron moves in strong fields and a variety of resonances (negative ion states) can be formed. Furthermore, the electronically excited state is often characterized by a change of the symmetry or of the total spin of the molecule. The probability for spin exchange via electron exchange is maximum when the velocity of the incident electron is comparable with the velocity of the bound electron. This effect, in general, leads to an increase of the excitation functions of spin-forbidden transitions at incident energies of several eV. Above this energy the probability for spin exchange decreases with increasing energy (Kuppermann *et al* 1979). However, this mechanism cannot explain the often very large cross sections of spin-forbidden transitions especially in the energy region from threshold to about 3 eV above.

A possible explanation for the behaviour of the cross section at low energies is an excitation via an intermediate shape or core-excited shape resonance, because these kinds of resonances typically exhibit broad peaks often of several hundreds meV FWHM in the cross sections. A concept useful for the description of these negative ion states is that of

0953-4075/96/040813+26$19.50

the formal capture of an electron by an electronic state of the neutral molecule, the parent state (for details see Ehrhardt and Frost 1993).

The potential energy curve of a shape resonance lies energetically above that of its parent state, which in this case is the ground state of the neutral molecule. A barrier is formed due to the centrifugal term $l(l+1)/r^2$ of the incoming electron altered by the non-spherical potential of the molecule. Therefore, the angular momentum l of the extra bond electron has to be $l \geqslant 1$. The parent state of a core-excited shape resonance is an electronically excited valence or a Rydberg state.

Although no core-excited shape resonances are known with the valence states of CO as parent states, recent calculations of Morgan and Tennyson (1993) predict six new resonances, three of symmetry $^2\Pi$ and one each of $^2\Sigma$, $^2\Delta$ and $^2\Phi$ symmetry. Especially the angular distribution measurements, which are performed here for the valence states of CO in this energy region for the first time, could verify the existence of three of these new resonances. It will be seen in the following that the decay of these new resonances together with that of the well known $^2\Pi$ shape resonance located at 1.8 eV is the dominating excitation mechanism for the lowest two triplet electronic states of CO in the threshold region.

This publication is the first of two publications about the electronic excitation of CO by electron impact near threshold. In this paper we present our measurements of the excitation from the ground state to various valence states of CO in comparison with several calculations with the aim of giving better insight into the excitation mechanism close to the threshold especially of spin-forbidden singlet $\rightarrow$ triplet transitions. The second publication deals with the excitation of Rydberg states of CO.

2. Apparatus

The measurements have been performed with a crossed beam spectrometer using tandem 127° cylindrical analysers for electron energy selection in an electron gun and detector (figure 1).

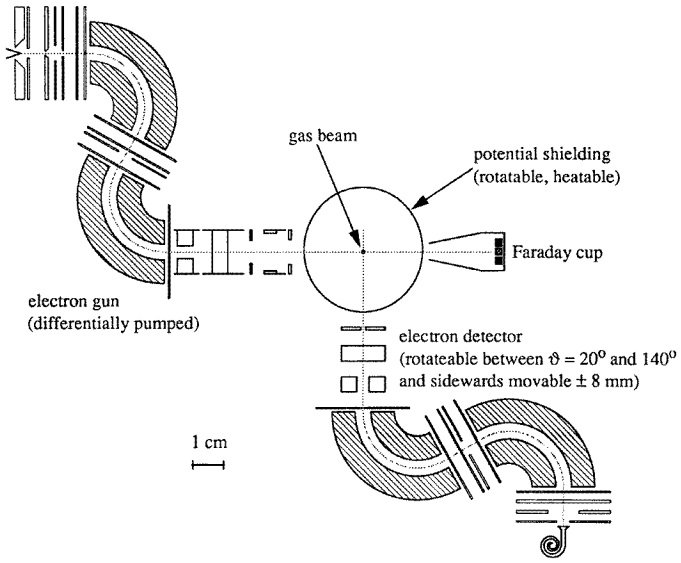

Figure 1. Schematic drawing of the crossed beam electron spectrometer.

The material used to build all elements is a special steel with extremely small magnetic field. A double shielding of μ-metal in combination with three pairs of Helmholtz coils placed perpendicular to each other reduces the residual magnetic field in the scattering region to lower than 0.5 mG.

The electron gun and the detector are heated during the measurements (190 °C and 120 °C) in order to reduce charging effects caused by contamination of the surfaces. The gas nozzle and the shielding of the scattering region are also heatable. The region with the highest electron density, i.e. the electron gun, is differentially pumped. During the measurements the partial pressure of the measured gas and the reference gas (here always helium) does not change because beside the gas under measurement the other gas is admitted into the chamber through a separate nozzle at a distance from the scattering region. This allows the stabilization (energy and intensity) of the spectrometer for several days. Aperture

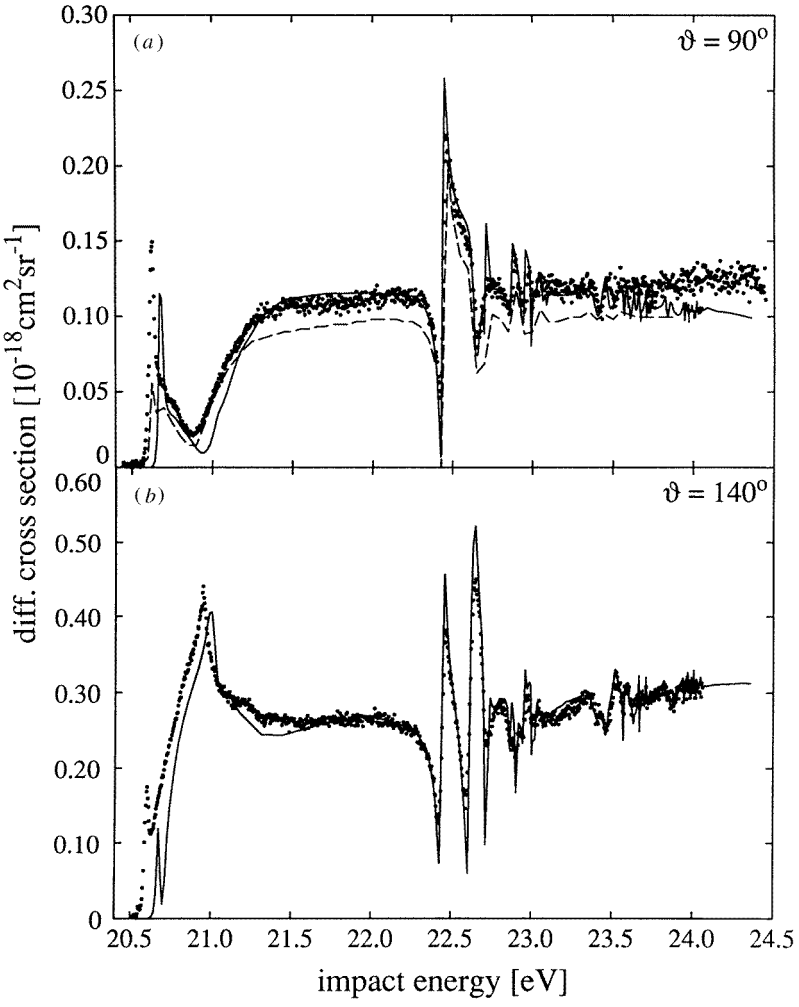

Figure 2. Differential excitation cross sections of He 2^1S at (*a*) 90° and (*b*) 140°. ——, Fon *et al* (1993); – – –, Allan (1992); ● , present result normalized to the calculated data of Fon at 22.2 eV.

lenses were used for all electron optical elements. It was found, especially for the entrance zoom optics of the detector, where electrons of very low energy have to be collected, that the disturbing influence of metal surfaces of this type of lens is minimum. The electron beam is controlled by a two-chamber Faraday cup. The multielement zoom optics of the electron gun are regulated by computer controlled digital to analogue converters. In order to ensure reliable measurements the electron beam has to be constant in intensity and spatial distribution over the measured range of energy.

The electron detector can be moved over an angular range from 0° to 140°. The overlap of the electron beam, the gas beam and the angle of view of the detector is controlled by an arrangement for the tangential movement of the detector with respect to the scattering volume over a range of ±8 mm at scattering angles between 20° and 120°. This enables us to control the spatial intensity distribution of the incident electron beam and to adjust it constant over an energy range from about 3.0 to 30 eV.

An overall energy resolution of 20 meV (FWHM) has been achieved. The shielding of the scattering region is rotatable to verify a homogenous electrostatic potential on its surface. Small voltages can be applied to the shielding and to the gas nozzle in order to compensate stray electric fields. These voltages just compensate the surface potential differences if the rise at threshold of the helium 2^1S state excitation function is very steep (see figures 2(*a*) and (*b*)), consistent with the fact, that the cross section at threshold is finite. From these measurements it was found that the accuracy of these potentials is better than 10 mV.

The energy scale is calibrated with respect to the ^{2}S resonance in the elastic cross section of helium at 19.36 eV and is accurate to ±0.03 eV. The absolute differential cross section of CO has been normalized with the relative flow technique (Srivastava *et al* 1975) and the reference data of the elastic cross section of helium (Nesbet 1979) at 3.7 eV.

3. Method

In principle, two kinds of measurements have been performed for the determination of absolute differential cross sections of the electronically excited states in CO, namely the measurement of angular dependences for constant impact energies and excitation functions at constant scattering angles.

For the determination of reliable angular dependences a novel measuring procedure was developed to ensure that at each angle the whole scattering volume, which is given by the overlap of the gas beam with the incident electron beam, is detected by the analyser. The essential point of this new approach, which in the following will be called the scanning method, is that we move the detector stepwise sidewards keeping the scattering angle fixed and take an energy loss spectrum at each position. Summing up the intensities for the different displacements we produce virtually a detector with a large uniform acceptance area, thus suppressing the undesired variation of the scattering volume with the angle. These measurements are possible in an angular range from 20° to 120°. The influence of the residual magnetic fields on the angular dependences could be estimated to be less then 5%. Together with the reproducibility of the measurements this will lead to total errors smaller than 12% for relative differential cross sections determined with this new method.

A further advantage of the possibility to move the detector sidewards is that the intensity profiles of the gas beam for different target molecules can be compared by taking the intensity profiles with identical electron beam and detecting conditions under a scattering angle of 90°. Thus it is possible to confirm that the gas flow conditions are identical for CO and helium within an error of 8%. This information is necessary to apply the relative flow method to get absolute cross sections.

To relate the collision dynamics to structures in the absolute differential cross section it is necessary to measure excitation functions knowing the detector transmission function as accurately as possible. This function has been controlled by measuring the nearly constant near-threshold ionization continuum of helium. It is finally obtained by subtracting the background, which is measured while CO and helium together are floating into the chamber through the separate gas nozzles. The detector transmission function was determined from threshold to 2.0 eV for scattering angles between 20° and 40° and from threshold to 3.7 eV from 50° to 140°.

Using classical trajectory calculations Wannier (1953) determined the energy dependence of the near-threshold total ionization cross section σ for the escape of two electrons from a singly ionized atom. He found σ to be proportional to $E_r^{1.127}$, where E_r is the excess energy. Considering only $(SL\pi) = {}^1S^e$ states (total angular momentum L, total spin S and parity π) of the final state two-electron wavefunction, a general consequence of the Wannier theory is a uniform distribution of the available energy E_r on the two outgoing electrons, leading to constant double-differential cross sections. The quantum mechanical confirmation of the Wannier theory was developed by Peterkop (1971) and by Rau (1971). Klar and Schlecht (1976) and later Greene and Rau (1982, 1983) removed the restriction of the Wannier theory to ${}^1S^e$ states. In the double differential cross section the influence of states with $L > 0$ will cause deviations from the uniformity in the energy dependence (see e.g. Fournier-Lagarde *et al* 1984, Read 1985). These deviations become more prominent with increasing excess energy. Therefore if one wants to use the ionization continuum to normalize the detector transmission function, the maximum excess energy E_r has to be known, up to which the influence of states with $L > 0$ is negligible, so that the energy dependence of the differential cross section still remains constant. Classical trajectory calculations of Read (1984) and measurements by Hammond *et al* (1985) of the cross section up to an incident energy of 0.6 eV above the ionization threshold of helium found the energy distribution to be flat within 5%. Selles *et al* (1987) found the triple differential cross sections for the ionization of helium at an energy $E_r = 2$ eV to be invariant with respect to different energy sharing of E_r to the two outgoing electrons leading to a constant energy distribution of the double differential cross section at each scattering angle (see also Hawley-Jones *et al* 1992). A similar result was found by Pichou *et al* (1978), who determined the double differential cross section to be flat up to $E_r = 2.4$ eV for scattering angles between 10° and 110°. Therefore the energy dependence of the double differential cross section for the ionization of helium is considered to be nearly constant at each scattering angle for $E_r \leqslant 2$ eV.

Clear deviations from the Wannier model were found in the work of Schubert *et al* (1981) and of Pichou *et al* (1978) at $E_r = 6.0$ eV and of Selles *et al* (1987) at $E_r = 8.0$ eV. To expand the measured energy range as wide as possible we have chosen E_r for our experiments between these energies and 2 eV, namely at $E_r = 3.7$ eV. At this excess energy it can be shown that the energy dependence of the differential ionization cross section is nearly constant for a scattering angle of 90°.

Comparison of the energy distributions taken at 90° with $E_r = 2$ eV and 3.7 eV show a similar energy dependence from threshold to a detecting energy of 2 eV. If we further consider that Pichou *et al* (1978), at nearly the same excess energy ($E_r = 3.6$ eV), found the energy distribution of the differential ionization cross section at 90° to be nearly constant for a detection energy from 0.8 to 3.6 eV, we can assume the energy dependence to be constant from threshold to $E_d = 3.7$ eV at this angle.

To determine the energy dependence of the differential ionization cross section at different scattering angles we carried out angular distribution measurements by using the scanning method in the whole detection energy range at $E_r = 3.7$ eV. These results could

than be normalized to the assumed constant differential cross section of the measurement at 90°.

Thus we obtain for $E_r = 3.7$ eV a variation partly much larger than 20% in the energy dependence of the relative differential ionization cross section of helium at scattering angles $\leqslant 40°$. The differential ionization cross sections at all other detected angles, which could be controlled by the scanning method, shows a flat energy dependence. As a consequence the detector transmission function for angles $\leqslant 40°$ could only be determined with $E_r = 2.0$ eV, for higher scattering angles we chose $E_r = 3.7$ eV. The values of CO at higher detection energies under angles $\leqslant 40°$ are determined by angular distribution measurements with the scanning method normalized to the absolute values at 90°.

The measured energy dependences at these small scattering angles were normalized to the absolute values of the measurements at 90° by determining the angular dependences of the differential cross sections with the scanning method at a residual energy of 1.8 eV. As written above it was possible to normalize the energy dependences at higher scattering angles to absolute values with the relative flow technique (Srivastava *et al* 1975) at a residual energy of 3.7 eV.

The error for relative excitation functions at one angle determined with this procedure is estimated to be less than 21%. Together with the error caused by the normalization to the helium elastic cross section this will lead to an error of 24% for the absolute values at detecting energies $\geqslant 200$ meV. The often strong increase of the detector efficiency at very low detecting energies causes the error for absolute values from threshold to 0.2 eV to be even higher. The regular operation of the apparatus has been tested by studying the rather well known transitions from the ground state of helium to the 2^3S and 2^1S states. Our results for the 2^1S state at detecting angles of 90° and 140° along with the corresponding data taken from a recent measurement of Allan (1992) and theoretical calculations of Fon *et al* (1992) are shown in figures 2(*a*) and (*b*). The agreement of the measurement at 140° with the calculation shows the applicability of the developed measurement procedure at scattering angles >120°, where the differential ionization cross sections cannot be controlled by the scanning method.

For comparison with available absolute cross sections we integrated our differential cross sections $d\sigma/d\vartheta$ following the equation $\sigma = 2\pi \int (d\sigma/d\vartheta) \sin\vartheta \, d\vartheta$. The missing angles to 0° and 180° are extrapolated from the measurements at 20° and 140°, respectively. The $\sin(\vartheta)$ factor in the integral reduces the contribution of the extrapolated values to the cross section and therefore the uncertainties caused by this extrapolation. The missing energy range for smaller angles from 2 to 3.7 eV above the threshold is extrapolated between the values determined with the scanning method. These values are marked with small circles in the presentation of the differential cross sections.

4. Results and discussion

The potential energy curves and the vibrational levels of the electronic states of CO up to the excitation energy of the E $^1\Pi$ state ($v = 0$ at 11.524 eV) are shown in figure 3. The *m* ($v = 0$ at 11.490 eV) and the *n* ($v = 0$ at 11.554 eV) states detected by Wallbank *et al* (1983) and by Hammond *et al* (1985) are not indicated. No potential curves exist for the d′ $^3\Delta$ ($v = 0$ at 9.81 eV), the b′ $^3\Pi$ ($v = 0$ at 9.324 eV) and the e′ $^3\Pi$ ($v = 0$ at 10.345 eV) states, which are suggested by Daviel *et al* (1982) by comparing their experimental data with energy loss spectra of the isoelectronic N_2 molecule.

A constant residual energy spectrum of the $e^- + CO$ system in the energy range from 5.9 to 11.7 eV taken with a detection energy E_d of 3.7 eV at 50° is shown in figure 4. The

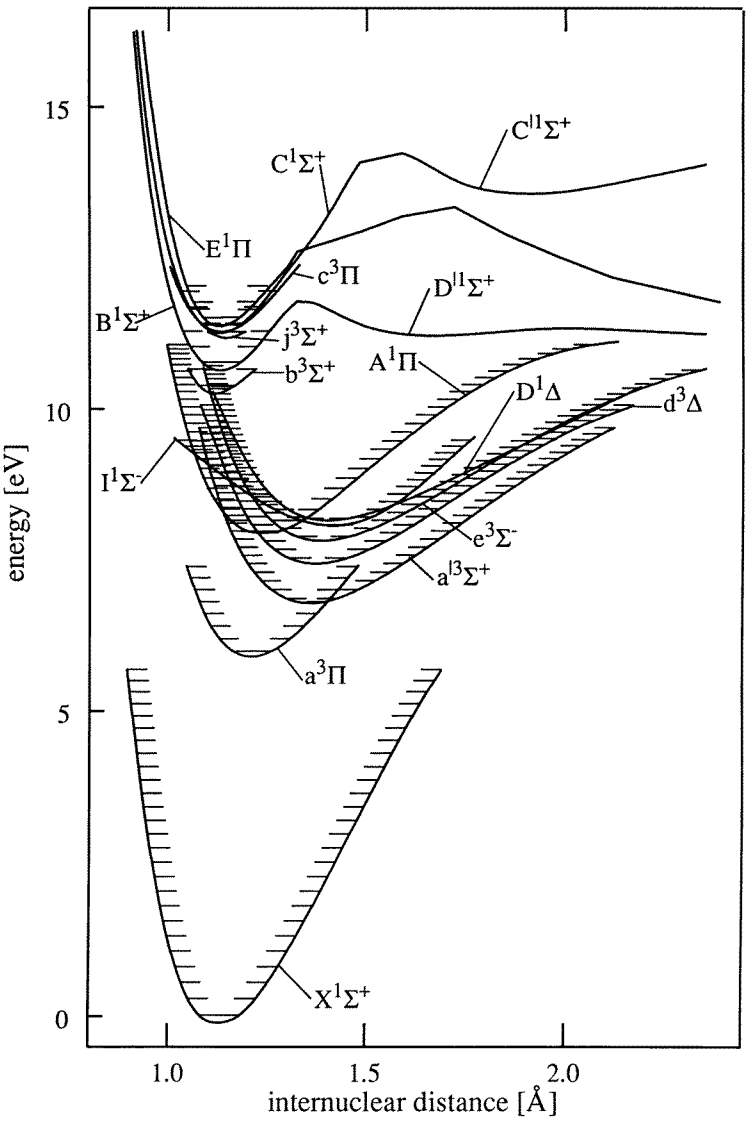

Figure 3. Potential energy curves and vibrational levels for electronic states of CO below 11.53 eV. Values taken from: X $^1\Sigma^+$, a $^3\Pi$, a′ $^3\Sigma^+$, d $^3\Delta$, I $^1\Sigma^-$, c $^3\Pi$ (Krupenie 1966); A $^1\Pi$, e $^3\Sigma^-$, D $^1\Delta$, b $^3\Sigma^+$, j $^3\Sigma^+$ (Tilford and Simmons 1972). Calculated potential energy curves of B $^1\Sigma^+$, D′ $^1\Sigma^+$, C $^1\Sigma^+$, C′ $^1\Sigma^+$, E $^1\Pi$ (Cooper and Kirby 1987) are shifted to the experimentally determined energy positions.

vibrational levels of the energetically separable states (values taken from Hammond *et al* 1985, Daviel *et al* 1982, Wallbank *et al* 1983) are marked in the figure. The arrow 1 indicates the excitation energy of the d $^3\Delta$ ($v = 17$) level at 9.611 eV. The e $^3\Sigma^-$, I $^1\Sigma^-$, D $^1\Delta$ and the D′ $^1\Sigma^+$ states are too low in intensity to be detected in this energy region. We also did not find indications for the d′ $^3\Delta$, b′ $^3\Pi$ and the e′ $^3\Pi$ states in the measured constant residual energy spectra.

The electronic structures and the energy positions of the electronic states below 11.53 eV

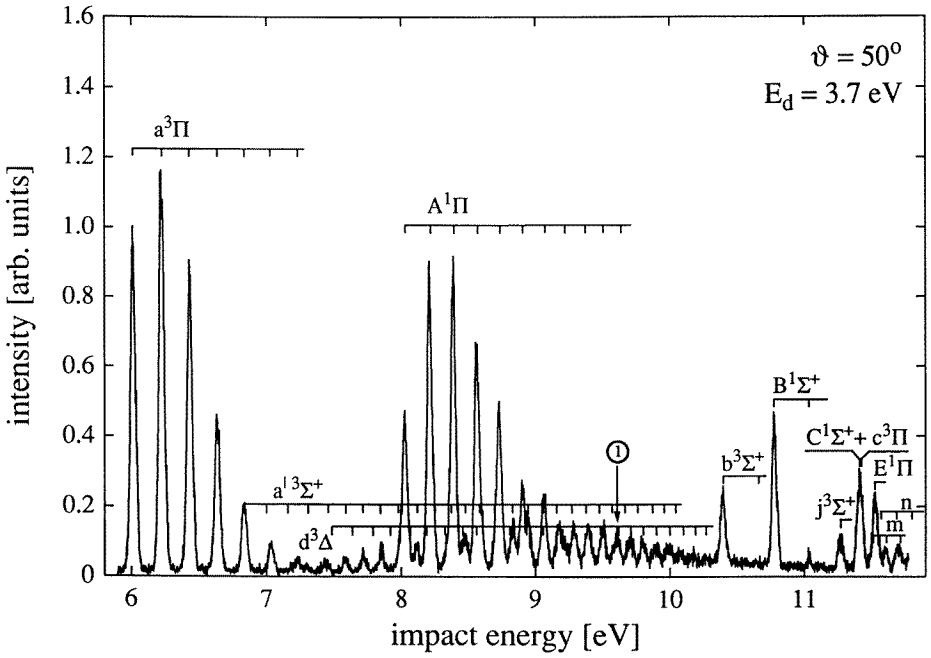

Figure 4. Constant residual energy spectrum of CO taken with a detection energy of 3.7 eV at a scattering angle of 50°.

are given in table 1 together with other relevant properties of these states. Orbital energy calculations of Huo (1966) and also of Chantranupong *et al* (1992) define the order of the orbitals for the ground state of CO with increasing energy leading to the configuration $1\sigma^2 2\sigma^2 3\sigma^2 4\sigma^2 1\pi^4 5\sigma^2$. The 1σ and 2σ core orbitals are expected to retain their atomic character during electronic excitation. From the remaining 10 valence electrons the lone pair orbitals 3σ and 4σ correspond to the 2s orbitals of the O and C atoms in the separated atom approximation. While the 1p and 5s orbitals possess bonding character the 2π and 6σ orbitals, which are not occupied in the ground state, are antibonding and delocalized (Kirby-Docken 1977). In the case of the a $^3\Pi$ state, where the 2π orbital is populated, the energetic order of the orbitals is changed (Huo 1966). Calculations of the orbital energies demonstrate that, for this state, the 5σ orbital is more tightly bound than the 1π orbital in contrast to the ground-state configuration.

In the following the measurements of valence states are discussed, which exhibit nominal intensities in the energy loss spectra, which are the a $^3\Pi$, the a′ $^3\Sigma^+$, the A $^1\Pi$ and the d $^3\Delta$ states. To our knowledge only three experimental groups have measured vibrationally resolved energy dependences close to the threshold of electronic transitions in CO. All three data sets are given in arbitrary units. The measurements of Swanson and co-workers (1975), which are taken at a scattering angle of 45°, will not be discussed in the following because, as the authors pointed out, they assume an unintended increase of the detector efficiency near zero energy. Although the detector transmission function is controlled very well by Allan (1989), a direct comparison of his results with our differential cross sections taken between 20° and 140° is impossible, because his trochoidal electron spectrometer (which he used at that time) only yields spectra being a sum of the differential cross sections at 0° and 180°. Excitation functions of the transition X $^1\Sigma^+$ ($v = 0$) → a′ $^3\Sigma^+$ ($v = 26$) in

Table 1. Electron configurations and the important properties of the vibrational level ($v = 0$) of electronic states of CO below 11.53 eV.

Electronic state	Electronic structure of CO: kl[a]	Valence orbitals: 1π	5σ	2π	6σ	Rydberg orbitals: 3σ	$3p\pi$	$3p\pi$	Energy of the $v' = 0$ vibrational level (eV)	Dipole moment (Debye)[b]	Equilibrium internuclear distance r_e (Å)[c]
X $^1\Sigma^+$	kl[a]	4	2	—	—	—	—	—[e]	0	0.112 ± 0.005[m]	1.128
a $^3\Pi$[d]	kl[a]	4	1	1	—	—	—	—[e]	6.006[i]	1.3740 ± 0.0003[n]	1.206
a′ $^3\Sigma^+$	kl[a]	3	2	1	—	—	—	—[e]	6.863[e]	$(-)1.06 \pm 0.2$[o]	1.352
d $^3\Delta$	kl[a]	3	2	1	—	—	—	—[e]	7.513[i]	$(-)0.42 \pm 0.02$[p]	1.369
e $^3\Sigma^-$	kl[a]	3	2	1	—	—	—	—[e]	7.898[j]		1.384
A $^1\Pi$	kl[a]	4	1	1	—	—	—	—[e]	8.024[i]	0.335 ± 0.013[q]	1.235
I $^1\Sigma^-$	kl[a]	3	2	1	—	—	—	—[e]	8.137[e]		1.391
D $^1\Delta$	kl[a]	3	2	1	—	—	—	—[g]	8.241[j]		1.399
b $^3\Sigma^+$	kl[a]	4	1	—	—	1	—	—[e]	10.399[k]	2.258[s]	1.113
B $^1\Sigma^+$	kl[a]	4	1	—	—	1	—	—[e]	10.777[k]	1.60 ± 0.15[r]	1.119
D′ $^1\Sigma^+$	kl[a]	3	2	1	—	—	—	—[h]	10.995[l]		
j $^3\Sigma^+$	kl[a]	4	1	—	—	—	1	—[f]	11.269[k]		1.144
C $^1\Sigma^+$	kl[a]	4	1	—	—	—	1	—[e]	11.396[k]	$(-)4.50 \pm 0.07$[q]	1.122
c $^3\Pi$	kl[a]	4	1	—	—	—	—	1[f]	11.414[k]		1.127
E $^1\Pi$	kl[a]	4	1	—	—	—	—	1[e]	11.524[k]		1.115

[a] kl describes the double occupied core orbitals $1\sigma^2 2\sigma^2 3\sigma^2 4\sigma^2$.
[b] Positive values indicate polarity C^+O^-.
[c] Huber and Herzberg (1979).
[d] Orbital energy calculations locate the 5σ orbital energetically below the 1π orbital for the a $^3\Pi$ state (Huo 1966).
[e] Krupenie (1966).
[f] Chung and Lin (1974).
[g] Rosenkrantz and Kirby (1989).
[h] Cooper and Kirby (1987).
[i] Daviel *et al* (1982) (experiment).
[j] Tilford and Simmons (1972) (experiment).
[k] Hammond *et al* (1985) (experiment).
[l] Wolk and Rich (1983) (experiment).
[m] Kopelman and Klemperer (1962) (experiment).
[n] Wicke and Klemperer (1975) (experiment).
[o] Wicke *et al* (1972) (experiment).
[p] Hemminger *et al* (1977) for ($v = 4$) (experiment).
[q] Drabbels *et al* (1993) (experiment).
[r] Fisher and Dalby (1976) (experiment).
[s] Calculated value of Weatherford and Huo (1990).

arbitrary units, measured by Mazeau *et al* (1972) from threshold to 0.5 eV above threshold, are discussed in comparison with our measurements at the end of this section.

Theoretical studies on electronic excitation of CO near threshold by electron impact have been recently reported by two groups. Morgan *et al* (1993) have reported *R*-matrix results for the cross sections of the lowest seven electronic transitions from threshold to 18 eV. The angular dependence of the differential cross section was determined only for the a′ $^3\Sigma^+$ state at 10.4 eV. Sun *et al* (1992) using the Schwinger multichannel variational method have reported both integral and differential cross sections for the excitation of the lowest electronically excited states for incident energies ranging from threshold to 30 eV. In addition to these results not yet published, calculations of McKoy *et al* (1994), also within the framework of the Schwinger multichannel variational method, will be compared with

the experimental results.

It has to be pointed out that all of these theoretical results are not vibrationally resolved. To compare the calculated cross sections with the experimentally determined ones, the measured differential cross sections of the different vibrational levels of the electronic state under study had to be summed. In the following figures, where the angular dependences of the cross sections are compared, the experimental results were summed for equal residual energies, because this method of summation corresponds most to the calculations. In contrast to this, the experimental results in the respective tables are vibrationally summed at fixed impact energies, which is a more standard format.

4.1. The a $^3\Pi$ *state*

The lowest electronically excited state of CO is the a $^3\Pi$ state. In this study we have measured the lowest six vibrational levels of this state. The vibrational levels $v = 0$, 1, 2 and 3 are clearly separated from other electronic transitions. As can be seen in figure 4 the vibrational levels 4 and 5 are superimposed by the $v = 0$ and $v = 1$ vibrational levels of the a′ $^3S^+$ state, but the intensity of this contribution is less then 20% of the two peaks.

The excitation functions from the ground state to the vibrational levels $v = 0$ to 5 of the a $^3\Pi$ state exhibit in the detected energy range from threshold to about 0.7 eV nearly the same relative shape. In this energy range the relative intensities of the levels are found to be 0.90, 1, 0.65, 0.31, 0.13, 0.04 which are almost in accordance with the calculated Franck–Condon factors (Halman *et al* 1965; 0.86, 1, 0.70, 0.38, 0.19, 0.10) for the direct, i.e. non-resonant, transition from the ground state to the a $^3\Pi$ state. This agreement is not necessarily an indication for non-resonant excitation: Huetz *et al* (1980) observed for the resonant excitation of the vibrational levels of the A $^3\Sigma_u^+$ state of N_2 intensities similar to the Franck–Condon factors. They found that this occurs if the width of the intermediate

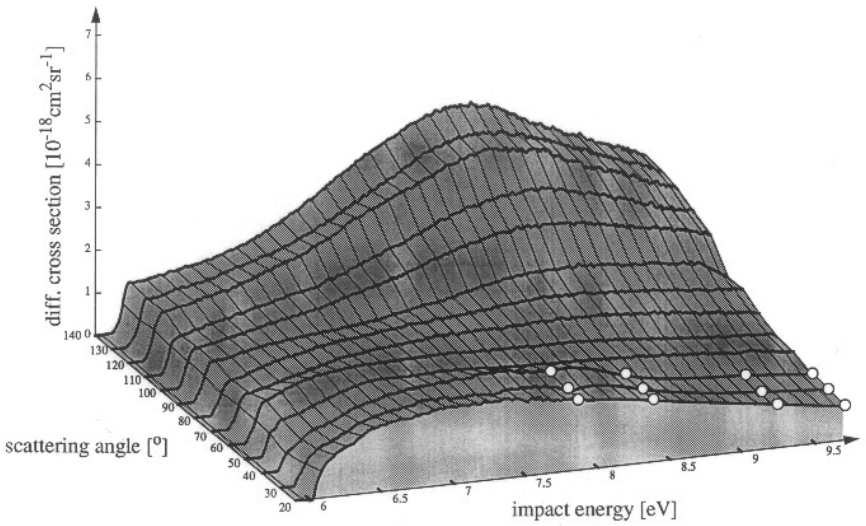

Figure 5. Energy dependence of the absolute differential cross sections for electronic excitation of the a $^3\Pi$ ($v = 0$) state of CO measured in the angular range from 20° to 140°. Below 50° and above 7.9 eV impact energy the differential cross sections is determined by angular distribution measurements (indicated by circles ○).

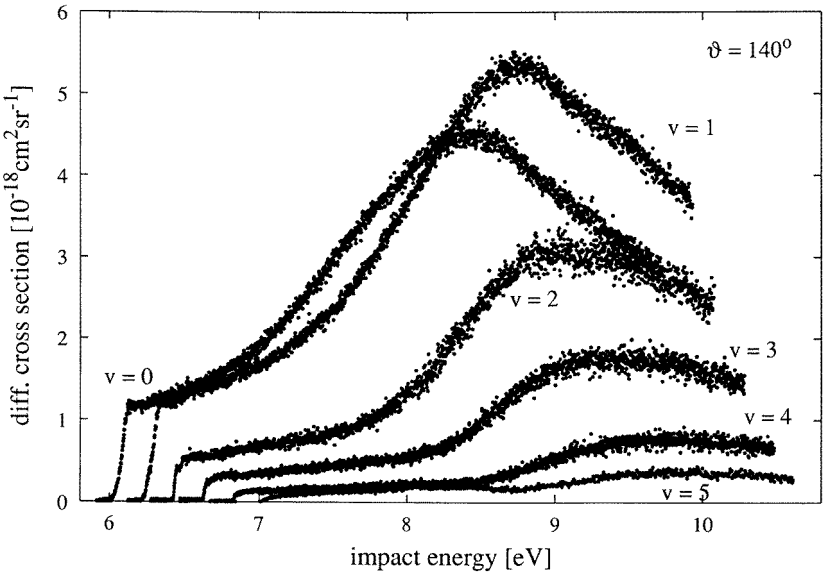

Figure 6. Energy dependences of the absolute differential cross sections of the transitions X $^1\Sigma^+$ ($v = 0$) $\rightarrow$ a $^3\Pi$ ($v = 0$–5) at 140°.

resonance state approaches a value for which the impulse limit model is valid.

Deviations from the Franck–Condon factors at impact energies of 10 and 15 eV already found by Trajmar *et al* (1971, 1973) in the relative cross sections of this transition indicate a resonant process at these energies. At 20 eV the relative intensities agree again with the Franck–Condon factors. As will become clear in the following, the reason for these deviations is resonances causing a broad peak in the differential cross section. It is exemplarily shown in the absolute differential cross sections of the X $^1\Sigma^+$ ($v = 0$) $\rightarrow$ a $^3\Pi$ ($v = 0$) transition (figure 5), that this broad peak (located here at about 8.5 eV) is more prominent at larger scattering angles. Selected absolute values of the differential cross section of the X $^1\Sigma^+ \rightarrow$ a $^3\Pi$ transition are summarized in table 2. Higher vibrational levels show similar differential cross sections (figure 6 for $\vartheta = 140°$). The peak becoming broader for higher vibrational levels is always found at comparable detection energies, which is consistent with the assumption that this feature is of resonant character. Information about the origin of the broad peak are provided by the analysis of the vibrationally summed ($v = 0$–5) integrated cross sections of the X $^1\Sigma^+ \rightarrow$ a $^3\Pi$ transition in comparison with available theoretical and experimental cross sections of other authors (figure 7(*a*)).

The broad peak is found in all curves presented in figure 7(*a*), but the energy position of the peak maximum as well as the FWHM differs in most of the results. The emission cross section measured by Ajello (1971) and the excitation cross section for metastable states of Newman *et al* (1983) involve cascading from energetically higher positioned triplet states. The latter measurement, given in arbitrary units, is normalized at 6.3 eV to our results, because this energy is below the $v = 0$ channel of the next triplet state (a′ $^3\Sigma^+$), which contributes to the measured intensity by decaying into the a $^3\Pi$ state. The steps which are visible at the threshold of the metastable excitation curve, and also in the present result, are caused by the opening of higher vibrational levels of the a $^3\Pi$ state. All other curves are not resolved with respect to vibrations, what is probably one reason for the discrepancies in the threshold energies. The sharp peak at 10.04 eV in the cross section of Newman *et al*

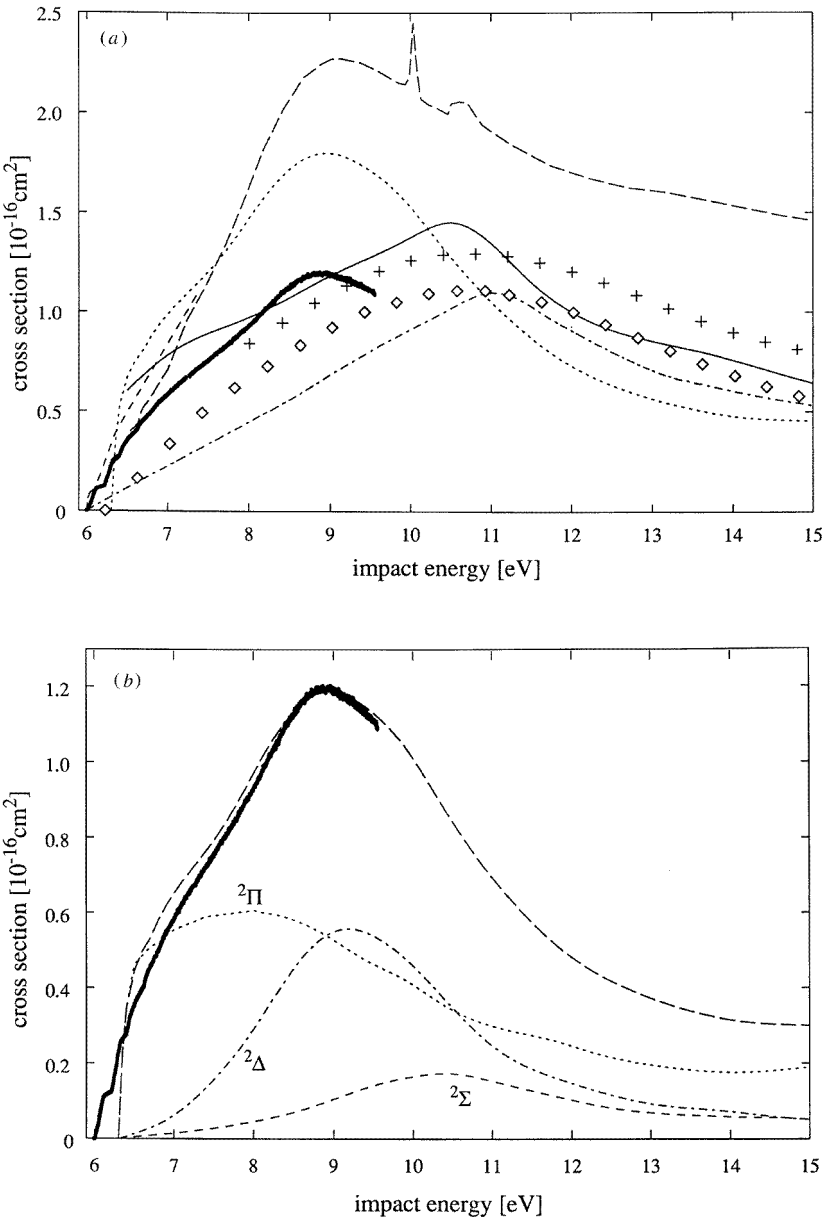

Figure 7. (*a*) Energy dependence of the integrated cross section of the transition X $^1\Sigma^+ \rightarrow$ a $^3\Pi$. ———, present result, summed over the vibrational levels $v = 0$–5. Calculations: ——, Sun *et al* (1992); · · · · · ·, Morgan and Tennyson (1993); +, Chung and Lin (1974). Absolute experimental data: — · —, Ajello (1971); – – –, Brongersma *et al* (1969); ◇, Land (1978). — — —, measurement of metastable states by Newman *et al* (1983) normalized at 6.3 eV to the present result. (*b*) Energy dependence of the integrated cross section of the transition X $^1\Sigma^+ \rightarrow$ a $^3\Pi$. ———, present result, summed over the vibrational levels $v = 0$–5; — — —, calculation of Morgan and Tennyson (1993) with resonant excitation via an intermediate (· · · · · ·) $^2\Pi$, (— · —) $^2\Delta$ and (– – –) $^2\Sigma$ resonance. These calculations are normalized to the experimental cross section at 8.8 eV.

Table 2. Absolute differential cross sections of the transition X $^1\Sigma^+ \rightarrow$ a $^3\Pi$. The vibrationally summed cross sections are taken at a constant incident energy E_i.

	ϑ												
E_i	20°	30°	40°	50°	60°	70°	80°	90°	100°	110°	120°	130°	140°
X $^1\Sigma^+$ ($v = 0$) → a $^3\Pi$ ($v = 0$), diff. cross section (10^{-18} cm^2 sr^{-1}), excitation threshold: 6.01 eV													
6.51	1.55	1.34	1.25	1.26	1.42	1.15	1.19	1.17	1.19	1.20	1.41	1.34	1.35
7.01	1.78	1.66	1.63	1.52	1.49	1.52	1.49	1.37	1.56	1.64	2.03	1.89	1.94
8.01					1.55	1.73	1.88	2.02	2.64	3.03	3.69	3.74	4.05
9.01					1.37	1.65	1.85	2.11	2.75	3.18	3.59	3.69	3.78
9.71	0.78	0.86	0.89	1.00	1.21	1.37	1.62	1.92	2.26	2.50	2.71	2.79	2.86
X $^1\Sigma^+$ ($v = 0$) → a $^3\Pi$ ($v = 1$), diff. cross section (10^{-18} cm^2 sr^{-1}), excitation threshold: 6.22 eV													
6.72	1.67	1.47	1.26	1.31	1.44	1.25	1.27	1.16	1.23	1.27	1.48	1.47	1.44
7.22	1.85	1.80	1.64	1.57	1.61	1.64	1.64	1.34	1.57	1.65	2.04	1.98	1.91
8.22					1.79	2.05	2.18	2.06	2.85	3.21	4.01	4.04	4.31
9.22					1.65	2.01	2.37	2.47	3.22	3.83	4.44	4.55	4.74
9.92	0.99	1.10	1.12	1.24	1.49	1.71	1.97	2.38	2.74	3.11	3.34	3.40	3.48
X $^1\Sigma^+$ ($v = 0$) → a $^3\Pi$ ($v = 0, 1, 2, 3, 4$ and 5), sum of the diff. cross sections (10^{17} cm^2 sr^{-1})													
6.5	0.34	0.28	0.25	0.26	0.29	0.24	0.26	0.25	0.25	0.25			0.32
7.0	0.55	0.46	0.43	0.42	0.42	0.42	0.43	0.39	0.43	0.45			0.47
8.0	0.44	0.41	0.38	0.36	0.52	0.57	0.62	0.60	0.74	0.83			1.00
9.0					0.53	0.64	0.74	0.81	0.99	1.16			1.43
9.5					0.49	0.61	0.71	0.79	0.96	1.10			1.32

(1983) is caused by the well known $^2\Sigma^+$ Feshbach resonance.

The overall shape of the present experimental curve is most similar to the calculation of Morgan and Tennyson (1993), and we have normalized this curve for better visual comparison to our absolute value at the peak maximum (8.8 eV) in figure 7(*b*). From this calculation it can be seen that the broad peak is suggested to be caused by a superposition of at least three resonant states, one each of $^2\Pi$, $^2\Delta$ and $^2\Sigma$ symmetry. Similar results are found by McKoy *et al* (1994) by a partial-wave analysis of a two-state calculated cross section. They determined the $^2\Pi$, $^2\Delta$ and $^2\Sigma$ contributions of the integrated cross section to be respectively 38.8%, 56.3% and 4.9% at an incident energy of 9.7 eV. No resonant states of $^2\Delta$ or $^2\Sigma$ symmetry have been found in CO at these energies before (maximum intensities at 9.2 eV for the $^2\Delta$ and 10.5 eV for the $^2\Sigma$ contribution, taken from the calculation of Morgan and Tennyson (1993)).

The angular distributions of the cross sections summed over the vibrations at equal detecting energies are compared with the only available angular dependences in figure 8: the five-state calculation of Sun *et al* (1992) (figures 8(*a*)–(*c*)) and the two-state calculation of McKoy *et al* (1994) in figure 8(*d*). At incident energies of 6.5 eV, 7.0 eV and 9.0 eV (figures 8(*a*)–(*c*)) the five-state calculations are in very good agreement with the measurements taken with detecting energies E_d of 0.5, 1.0 and 3.0 eV, while the two-state calculation at 9.7 eV ($E_d = 3.7$ eV) shows a similar overall shape of the angular distribution, but overestimates the absolute value of the experimental values in the backward scattering direction.

Regarding the electron configuration of the a $^3\Pi$ state to be $kl\,1\pi^4 5\sigma^1 2\pi^1$, the electron configuration for the energetic lowest core-excited shape resonances with this parent state is found by adding a further 2π electron, giving rise to two resonances of $^2\Sigma^+$ symmetry and one each of $^2\Sigma^-$, $^4\Sigma^+$ and $^2\Delta$ symmetry (Massey *et al* 1969), in agreement with the

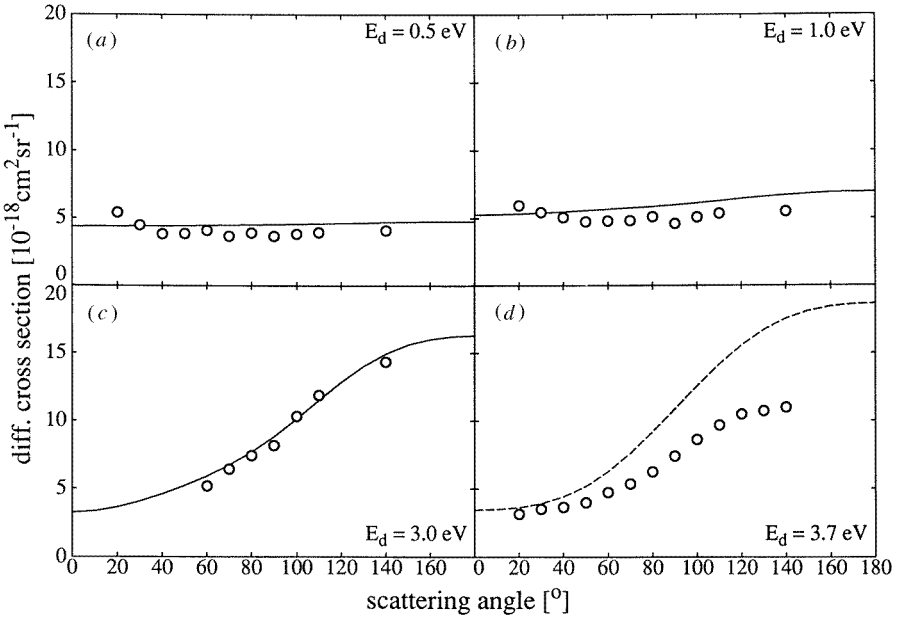

Figure 8. Angular dependence of the vibrationally summed (v = 0–5) cross section of the X $^1\Sigma^+ \rightarrow$ a $^3\Pi$ transition. ○, present results, summed at equal residual energies; ——, five-channel calculation of Sun *et al* (1992); — — —, two-channel calculation of McKoy *et al* (1994). Incident energies (for $v = 0$): (*a*) 6.5 eV, (*b*) 7.0 eV, (*c*) 9.0 eV, (*d*) 9.7 eV.

suggested symmetries of the new resonances. The decay of the $^2\Sigma$ and $^2\Delta$ resonances into their parent state is possible without a spin flip or spin exchange by ejecting a 2π electron with a different spin than the incoming electron.

A second remarkable feature in common for all vibrational levels of the X $^1\Sigma^+ \rightarrow$ a $^3\Pi$ transition is the sharp rise in the cross sections just at the threshold (see figures 5 and 6), suggesting that there exists a resonant state at this energy. The determination of the width of this ascent is limited by the experimental energy resolution and is found to be smaller than 40 meV.

Following the calculation of Morgan and Tennyson (1993) as well as from the calculation of McKoy (1994), the symmetry of the resonant state mainly contributing to the cross section of the X $^1\Sigma^+ \rightarrow$ a $^3\Pi$ transition in the energy range from threshold to about 1 eV is $^2\Pi$. Morgan and Tennyson (1993) attributed this resonant feature to be caused by the far wing of the $^2\Pi$ shape resonance at 1.8 eV (Ehrhardt *et al* 1968). The large coverage of this resonance can also be seen in the measurements of the vibrational excitation of the ground state of CO (Allan 1989), where the influence of the resonance still dominates the cross section of the highest measured vibrational level ($v = 15$) at about 4.3 eV impact energy.

The electron configuration of the discussed $^2\Pi$ shape resonance is $kl\ 1\pi^4 5\sigma^2 2\pi^1$ with a 2π electron attached to the ground state, and therefore the decay into the a $^3\Pi$ state requires the ejection of a 5σ electron. Similar to the decay of the two core-excited shape resonances $^2\Sigma$ and $^2\Delta$, the triplet character of the final state requires the spin of the ejected electron to be antiparallel to the incident one.

Close to the threshold of the a $^3\Pi$ state at 6.5 and 7 eV incident energy (figures 8(*a*), (*b*)) the angular behaviour of the scattered electrons is found to be isotropic (except for a small rise in forward direction below 40°). This is characteristic of an sσ partial wave.

A similar angular behaviour at threshold was calculated by Sun *et al* (1992). Considering the symmetry $\Lambda = 1$ of the a $^3\Pi$ state and supposing pure resonant excitation one has to assume from the measured as well as from the calculated angular behaviour the intermediate resonance state to be of Π symmetry. This is in agreement with the analysis of the integrated cross section of Morgan and Tennyson (1993) and of McKoy *et al* (1994). Therefore, the excitation mechanism, which will be called in the following the 'multichannel resonant decay mechanism', in the case of the a $^3\Pi$ state is

$$\mathrm{X}\ ^1\Sigma^+(\Lambda = 0) + \mathrm{e}^-(l_{\min} = 1, \lambda = 1) \rightarrow {}^2\Pi(\Lambda = 1) \rightarrow \mathrm{a}\ ^3\Pi(\Lambda = 1) + \mathrm{e}^-(l_{\min} = 0, \lambda = 0)$$

where Λ and λ are the projections of the angular momentum of the molecule and of the electron on the internuclear axis, and $l_{\min}$ is the minimal angular momentum of the electron, necessary for this excitation process.

For the first time Chang (1977) proposed an excitation via a resonance far below the final state for the lowest two electronically excited states of O_2, but he did not give an explanation for the strong influence of a resonance over more than 4 eV. A detailed analysis of the electronic excitation of the lowest electronically excited states of O_2 (Teillet-Billy *et al* 1987, 1989) using the multichannel effective range theory determined the low-lying $^2\Pi_g$ resonance of O_2 as the intermediate compound state for the resonant electronic excitation, thus confirming the interpretation of Chang (1977).

The long-range influence of a resonance can be calculated following the evaluation of the Breit–Wigner formula. The decay probability $\Gamma(E)/\hbar$, even several eV above a resonance, can be determined from the formula (Joachain 1975):

$$\Gamma(E) = \frac{(ka)^{2l+1}}{((2l-1)!!)^2}\left(\frac{h^2}{2\pi^2 m \mathrm{a}^2}\right)$$

where E is the energy of the incident electron, k is the wavenumber of the incident electron, a is the range of the scattering potential, l is the angular momentum of the electron, h is the Planck constant and m is the mass of the electron.

With $k^2 = 8E\pi m/h^2\Gamma(E)$ therefore follows the Wigner threshold law:

$$\Gamma(E) = E^{(l+1/2)}$$

(see also the determination of the width $\Gamma(E)$ of the $^2\Pi_g$ resonance in O_2 by Teillet-Billy *et al* 1987). Only if the incident energy is close to the resonance position, $\Gamma(E)$ approaches the measured FWHM of the resonance. Furthermore, if there is more than one decay channel for the resonance as in the case of multichannel resonant decay, the total width of the resonance is determined by the sum of the partial resonance widths in the respective decay channels.

In contrast to the work of Teillet-Billy *et al* (1987, 1989), who analysed only the integrated cross section of the electronic excitation, in our case the determination of the contributing partial waves by comparing the measured angular dependences with calculated differential cross sections and, furthermore, the analysis of the integrated cross section clearly supports the assumption of the excitation of the a $^3\Pi$ state via the $^2\Pi$ shape resonance located at 1.8 eV.

Therefore the multichannel resonant decay mechanism allows population of states of even different symmetries and different total spins via the decay of a shape resonance by ejecting electrons more tightly bounded than those in the highest populated molecular valence orbital of the resonance.

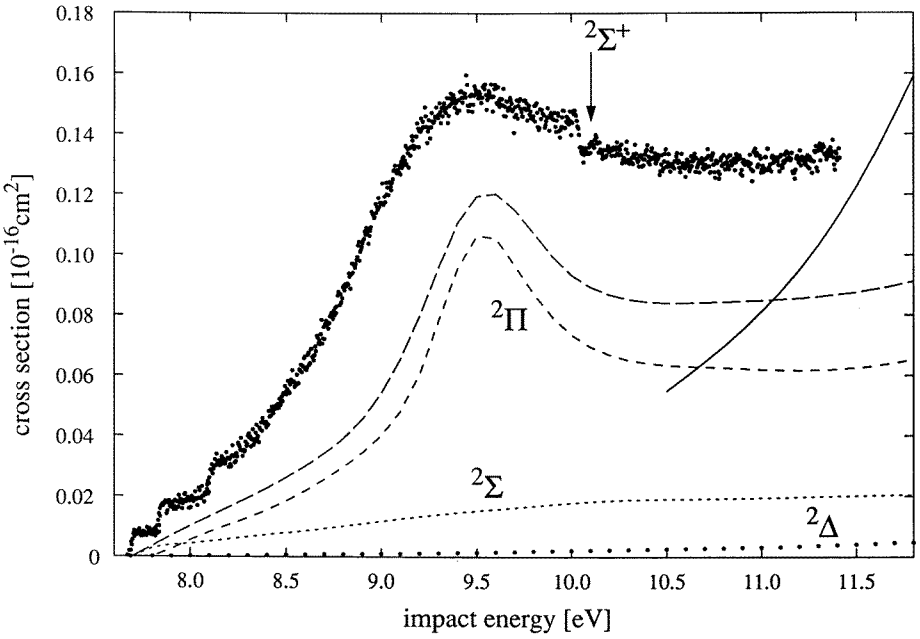

Figure 9. Energy dependence of the integrated cross section of the transition X $^1\Sigma^+ \rightarrow$ a′ $^3\Sigma^+$. ● , present result, summed over the vibrational levels $v = 6$, 7 and 9 and divided by the sum of the respective Franck–Condon factors (0.1954; Krupenie 1966); ——, calculation of Sun *et al* (1992); — — —, calculations of Morgan and Tennyson (1993) shifted to the experimental threshold energy with resonant (– – –) $^2\Pi$, (· · · · · ·) $^2\Sigma$ and (· · · · · ·) $^2\Delta$ contribution.

4.2. The a′ $^3\Sigma^+$ *state*

The vibrational levels of the X $^1\Sigma^+$ ($v = 0$) $\rightarrow$ a′ $^3\Sigma^+$ transition are indicated in the energy-loss spectrum (figure 4). Because of the lack of intensity and the overlap of several vibrational levels of the a′ $^3\Sigma^+$ state with those of other electronic states it was only possible to measure the vibrational levels $v = 6$, 7 and 9. The differential cross sections of these vibrational levels exhibit a small but steep rise at the threshold, which is visible in the vibrationally summed integrated cross section of the X $^1\Sigma^+$ ($v = 0$) $\rightarrow$ a′ $^3\Sigma^+$ ($v =$ 6, 7 and 9) transitions (figure 9). Absolute values for the differential cross sections of this transitions are given in table 3.

Sun *et al* (1992) found in their calculation substantial dπ wave contribution in the outgoing channel at energies from threshold to 30 eV. The same dominating partial wave is found in all measured vibrational transitions 100 meV above their thresholds by comparing the measured angular dependences with a dπ partial wave. This behaviour is shown exemplarily for the transition X $^1\Sigma^+$ ($v = 0$) $\rightarrow$ a′ $^3\Sigma^+$ ($v = 6$) in figure 10(*a*). A possible explanation for this angular distribution as well as for the steep rise at threshold in the excitation function of the a′ $^3\Sigma^+$ state is, analogous to the case of the a $^3\Pi$ state, a resonant excitation via a $^2\Pi$ resonance located below the threshold of the a′ $^3\Sigma^+$ state. The only candidate known from experimental or theoretical studies which satisfies this condition is again the low-lying $^2\Pi$ resonance located at 1.8 eV with the electron configuration $kl\,1\pi^4 5\sigma^2 2\pi^1$. In contrast to the decay into the a $^3\Pi$ state where a 5σ electron has to be ejected from this $^2\Pi$ resonance, in this case a 1π electron has to be ejected. This is in agreement with the measured angular distribution of a dπ scattering wave just at threshold.

Table 3. Absolute differential cross sections of the transition X $^1\Sigma^+ \rightarrow$ a′ $^3\Sigma^+$.

	ϑ												
E_i	20°	30°	40°	50°	60°	70°	80°	90°	100°	110°	120°	130°	140°
X $^1\Sigma^+$ ($v = 0$) → a′ $^3\Sigma$ ($v = 6$), diff. cross section (10^{-18} cm^2 sr^{-1}), excitation threshold: 7.71 eV													
7.81	0.026	0.020	0.007	0.009	0.009	0.009	0.015	0.017	0.012	0.011	0.008	0.011	0.012
9.01	0.161	0.143	0.091	0.081	0.069	0.041	0.038	0.034	0.037	0.042	0.048	0.061	0.058
9.51	0.142	0.122	0.097	0.072	0.067	0.043	0.043	0.040	0.042	0.043	0.048	0.059	0.061
11.41	0.093	0.078	0.075	0.054	0.048	0.040	0.044	0.046	0.044	0.047	0.05	0.043	0.042
X $^1\Sigma^+$ ($v = 0$) → a′ $^3\Sigma$ ($v = 6, 7$ and 9), sum of the diff. cross sections (10^{18} cm^2 sr^{-1})													
9.0	0.594	0.459	0.278	0.261	0.178	0.120	0.106	0.092	0.104	0.113	0.148	0.166	0.160
10.0					0.272	0.223	0.172	0.168	0.156	0.149	0.174	0.184	0.189
11.0					0.211	0.181	0.148	0.156	0.180	0.176	0.188	0.177	0.167

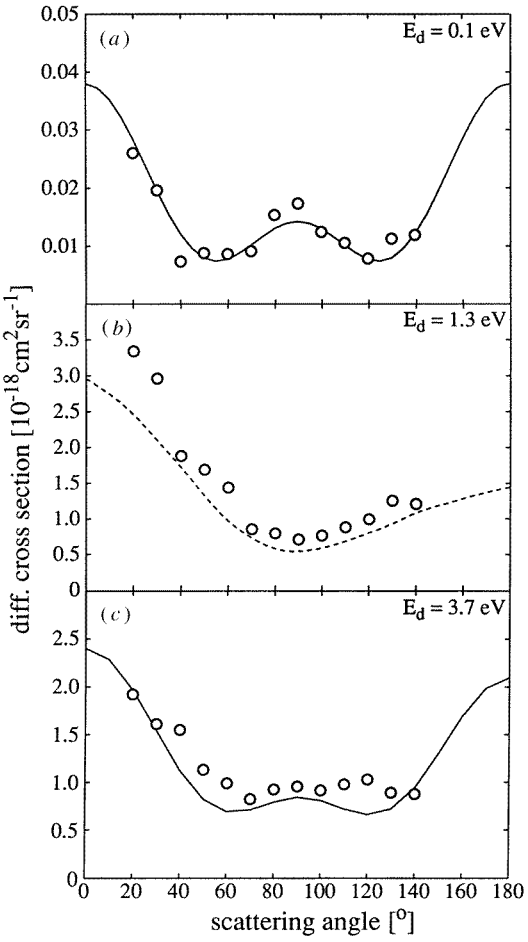

Figure 10. Angular dependence of the differential cross section of the X $^1\Sigma^+$ ($v = 0$) → a′ $^3\Sigma^+$ ($v = 6$) transition at different detecting energies. (*a*) ○, present result at a detection energy $E_d = 0.1$ eV; ——, angular distribution of a dπ scattering wave (Read 1968) normalized to the present data at 30°. (*b*) ○, present result at $E_d = 1.3$ eV divided by the Franck–Condon factor (0.0483; Krupenie 1966); - - - -, calculation of Morgan and Tennyson (1993) at $E_d = 1.9$ eV. (*c*) ○, present results at $E_d = 3.7$ eV divided by the Franck–Condon factor (0.0483; Krupenie 1966); ——, calculation of Sun *et al* (1992) at $E_d = 3.56$ eV.

In contrast to our results, the dominating resonant contribution to the cross section at very low detecting energies found by Morgan and Tennyson (1993) is $^2\Sigma$ as visible in figure 9. Of course, the differential cross section at the threshold of the a′ $^3\Sigma^+$ state is much smaller than that of the a $^3\Pi$ state, because the ejection of a more tightly bonded electron is less

probable (see also the excitation of O_2 in Teillet-Billy *et al* 1989). The excitation mechanism at the threshold of the $a'\ ^3\Sigma^+$ state via the $^2\Pi$ (1.8 eV) resonance is therefore described as a multichannel resonant decay mechanism.

At higher detection energies we found a different dominating resonant excitation mechanism.

The differential cross section of the $X\ ^1\Sigma+\ (v=0) \rightarrow a'\ ^3\Sigma^+\ (v=6)$ transition exhibits at energies of about 1.3 eV above the threshold a broad hump towards larger and smaller angles. The measured differential cross sections of the vibrational $v = 7$ and 9 levels show similar shapes with the difference that the position of the hump is shifted to higher impact energies with similar energy spacings to the energy differences between the respective vibrational levels. This behaviour supports the assumption of a resonant feature at this energy. The lowest core-excited shape resonance with the $a'\ ^3\Sigma^+$ state as the parent state is built by adding the extra electron in a 2π orbital of the $a'\ ^3\Sigma^+$ state. This leads to an electron configuration $kl\ 1\pi^3 5\sigma^2 2\pi^2$ giving rise to three resonances of $^2\Pi$ and one each of $^4\Pi$ and $^2\Phi$ symmetry (Massey *et al* 1969). The angular distribution measured at 1.3 eV above the threshold of the $a'\ ^3\Sigma^+\ (v=6)$ state is given in figure 10(*b*) in comparison with the calculation of Morgan and Tennyson (1993) at 10.4 eV. As pointed out before, the calculations are not vibrationally resolved and therefore we divided the measured differential cross section by the respective Franck–Condon factor taken from Krupenie (1966). The measured as well as the calculated distribution show the behaviour of a dominating resonant $p\pi$ wave interfering with a $d\pi$ wave. In contrast to the excitation of the $a\ ^3\Pi$ state, where three resonances of different symmetries contribute to the excitation at higher energies, in this case we find an isolated resonance dominating the excitation. Regarding the symmetries of the initial and final state, both are of Σ^+ symmetry, together with the measured angular distribution one can conclude, that the intermediate resonance has to be of Π symmetry (Read 1968). The only previous indication of a $^2\Pi$ resonance with the electron configuration $kl\ 1\pi^3 5\sigma^2 2\pi^2$ was given by Hall *et al* (1977) in the cross section for dissociative attachment in CO. They found that the lowest dissociative electron capture process, which is possible above the threshold at 9.62 eV, proceeds via an intermediate $^2\Pi$ resonance state in the form

$$CO(X\ ^1\Sigma^+) + e^- \rightarrow CO^{*-}(^2\Pi) \rightarrow O^-(^2P) + C(^3P)$$

This $^2\Pi$ resonance causes a strong peak in the calculated cross section of the $X\ ^1\Sigma^+ \rightarrow a'\ ^3\Sigma^+$ transition (Morgan and Tennyson 1993) at an energy of 1.9 eV above the threshold. In figure 9 the vibrationally not-resolved calculated data are compared with the vibrationally summed ($v = 6$, 7 and 9) integrated cross section of the present study (divided by the sum of the respective Franck–Condon factors for better visual comparison). A small difference in the position of the resonance and a larger FWHM of the experimentally found feature is obvious. It has to be noticed that the FWHM of this hump would be enlarged if all vibrational levels were to be summed up. For a single vibrational transition the FWHM of the resonance is estimated to be 1.2 ± 0.3 eV, while the calculated width of the new $^2\Pi$ resonance is about 0.15 eV (taken from figure 3 of Morgan and Tennyson (1993) at the equilibrium distance of the $a'\ ^3\Sigma^+$ state $r_e = 1.352$ Å). The cross sections calculated by the same authors for resonant $^2\Pi$, $^2\Delta$ and $^2\Sigma$ excitation are also given in figure 9. The $^2\Delta$ and $^2\Sigma$ contributions are small and exhibit no typical resonant structures, according to the fact that we did not find any indications for the influence of a $^2\Delta$ or a $^2\Sigma$ core-excited shape resonance on the cross section of the $a'\ ^3\Sigma^+$ state. The integrated cross section of Sun *et al* (1992) is shown in the same figure, and strong differences are found to the experimentally determined shape of the cross section and to the calculation of Morgan and Tennyson (1993).

However, at a detection energy of 3.7 eV (figure 10(*c*)) the measured angular distribution has changed to a form similar to that calculated by Sun *et al* (1992) at a detection energy equal to 3.56 eV, indicating that at this energy the influence of the new resonance is of minor importance.

Both theoretical calculations do not reflect the $^2\Sigma^+$ Feshbach resonance at 10.04 eV (figure 9). The intensity of the structure is rather small because a decay of this resonance to the a′ $^3\Sigma^+$ state is only possible by configuration mixing (Pearson and Lefebvre-Brion 1976).

4.3. The A $^1\Pi$ *state*

The lowest dipole-allowed electronic transition in CO is the so-called fourth positive system, the X $^1\Sigma^+ \rightarrow$ A $^1\Pi$ transition. As can be seen in figure 4, the different vibrational bands are overlapping with the vibrational levels of the a′ $^3\Sigma^+$ and d $^3\Delta$ states because of the limited energy resolution. The contribution of these states to the lowest five vibrational levels of the A $^1\Pi$ state, which have been measured here, is estimated to be less than 20%. Similar for all measured vibrational transitions the differential cross section starts at threshold with a value of zero and shows a nearly continuous rise with the incident energy. Except for an energy region from threshold to a detecting energy of about 200 meV, where the differential cross section is found to be isotropic (see also table 4), at higher detecting energies a strong increase of the differential cross sections is found for decreasing scattering angles, typical for a dipole-allowed transition. Clearly visible is the strong interference structure of the well known $^2\Sigma^+$ ($v = 0$) Feshbach resonance at 10.04 eV. In contrast to the spin-forbidden transitions discussed above, no indications are found for resonant scattering in the angular behaviour of the vibrationally summed (v = 0–4) differential cross sections (figure 11).

Table 4. Absolute differential cross sections of the transition X $^1\Sigma^+ \rightarrow$ A $^1\Pi$.

	ϑ												
E_i	20°	30°	40°	50°	60°	70°	80°	90°	100°	110°	120°	130°	140°
X $^1\Sigma^+$ ($v = 0$) → A $^1\Pi$ ($v = 0$), diff. cross section (10^{-18} cm^2 sr^{-1}), excitation threshold: 8.02 eV													
8.52	0.16	0.159	0.097	0.088	0.071	0.059	0.062	0.054	0.053	0.048	0.063	0.070	0.094
9.02	0.38	0.28	0.18	0.20	0.14	0.12	0.11	0.10	0.10	0.10	0.12	0.12	0.17
9.82	0.64	0.47	0.36	0.29	0.22	0.18	0.18	0.16	0.17	0.17	0.18	0.19	0.20
10.52					0.31	0.24	0.23	0.21	0.22	0.22	0.24	0.24	0.27
11.02					0.37	0.30	0.27	0.24	0.27	0.25	0.25	0.25	0.26
11.72	1.47	1.13	0.79	0.53	0.41	0.33	0.32	0.31	0.34	0.33	0.34	0.32	0.29
X $^1\Sigma^+$ ($v = 0$) → A $^1\Pi$ ($v = 2$), diff. cross section (10^{-18} cm^2 sr^{-1}), excitation threshold: 8.39 eV													
8.89	0.31	0.30	0.19	0.17	0.11	0.11	0.12	0.11	0.10	0.09	0.12	0.14	0.16
9.39	0.73	0.55	0.36	0.39	0.25	0.22	0.22	0.20	0.20	0.19	0.28	0.30	0.31
10.19	1.17	0.92	0.74	0.58	0.44	0.39	0.37	0.35	0.35	0.36	0.37	0.42	0.43
10.89					0.57	0.46	0.42	0.41	0.41	0.41	0.44	0.44	0.44
11.39					0.73	0.56	0.55	0.55	0.58	0.50	0.54	0.52	0.50
12.09	2.75	2.09	1.33	0.95	0.73	0.62	0.55	0.57	0.59	0.61	0.60	0.53	0.50
X $^1\Sigma^+$ ($v = 0$) → A $^1\Pi$ ($v = 0, 1, 2, 3$ and 4), sum of the diff. cross sections (10^{18} cm^2 sr^{-1})													
8.5	0.30	0.32	0.24	0.23	0.16	0.16	0.18	0.16	0.15	0.13	0.13	0.17	0.20
9.0	1.72	1.34	0.86	0.81	0.57	0.51	0.55	0.50	0.49	0.44	0.59	0.67	0.73
10.0	3.43	2.77	2.18	1.97	1.86	1.56	1.52	1.39	1.44	1.49	1.67	1.77	1.92
11.0					2.35	1.89	1.76	1.76	1.72	1.71	1.75	1.80	1.78
11.5					2.89	2.32	2.26	2.23	2.38	2.19	2.12	2.14	2.06

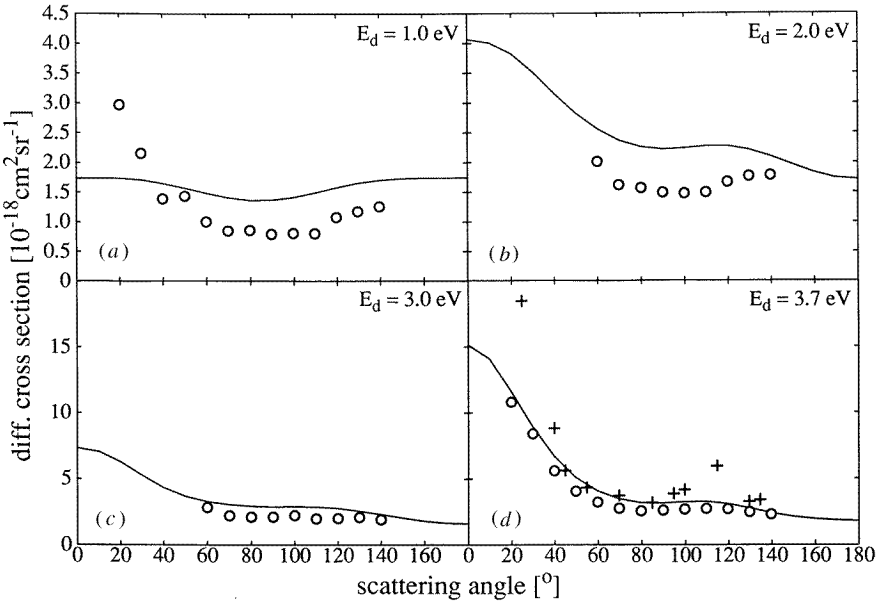

Figure 11. Angular dependence of the vibrationally summed (v = 0–4) cross section of the X $^1\Sigma^+ \rightarrow$ A $^1\Pi$ transition. ○, present result, summed at equal residual energies; ——, calculation of Sun *et al* (1992). (*a*) detection energy E_d = 1 eV in comparison with the calculation at an incident energy E_c = 10.5 eV, (*b*) E_d = 2.0 eV, E_c = 11.5 eV, (*c*) E_d = 3.0 eV, E_c = 12.5 eV, (*d*) E_d = 3.7 eV, E_c = 13.5 eV; +, preliminary experimental results of Trajmar (1994) detected at E_c = 12.5 eV.

For comparison with the calculations of Sun *et al* (1992) the values of the measured differential cross sections at the corresponding detection energies above the threshold of each vibrational level have been summed. The energy positions of the calculated angular dependences are shifted about 1 eV to lower energies to bring the calculated threshold of this transition (9.52 eV) in agreement with the averaged threshold of the vibrational bands at 8.5 eV. At low detection energies (figures 11(*a*) and (*b*)) strong differences to the calculations, especially in forward scattering direction, are found. The agreement improves with increasing energies. At higher energies (figure 11(*d*)) the calculation predicts the experimental findings and only slightly overestimates the measured cross sections. The preliminary experimental results of Trajmar (1994), which are—in contrast to our results—vibrationally summed at one fixed incident energy (12.5 eV), show deviations to our values especially in the forward scattering direction.

In figure 12 the sum of the integrated cross sections of the vibrational levels v = 0–4 is shown along with the available cross sections of other groups. The calculation of Sun *et al* (1992) is again shifted to the averaged threshold of the vibrational bands at 8.5 eV. Except for the vibrationally (v = 0–4) summed experimental result of Mumma *et al* (1971) and the calculation of Sun *et al* (1992), which are both not given close to the threshold, all curves show a very smooth onset at threshold followed by a continuous increase of the cross section. The calculation of Sun *et al* (1992) and that of Morgan and Tennyson (1993) seem to overestimate the absolute value of the total cross section by only about 10%–20%. A reason for this rather small deviation may be on the one hand the disregarding of higher electronically excited states in the calculation, which reduces the flux of incident electron

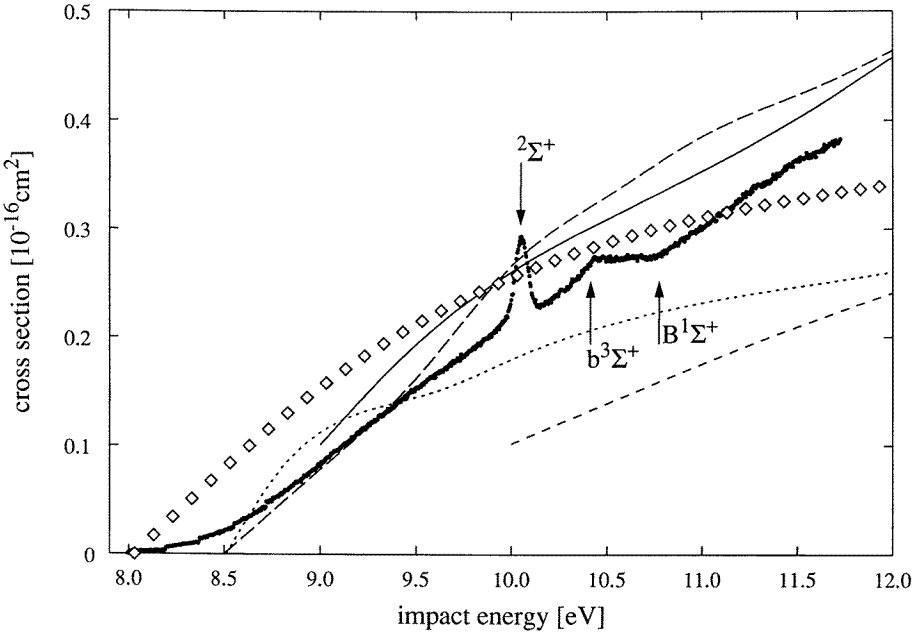

Figure 12. Energy dependence of the integrated cross section of the transition X $^1\Sigma^+ \rightarrow$ A $^1\Pi$. ———, present result, summed over the vibrational levels $v = 0$–4. Calculations of: ——, Sun *et al* (1992); — — —, Morgan and Tennyson (1993). Absolute experimental data of: – – –, Mumma *et al* (1971) - - - -, Land (1978); ◊, Ajello (1971).

intensity by offering alternative excitation channels. On the other hand there is a small contribution of vibrational levels higher than $v = 4$, which has to be added to our integrated cross section.

Neither in the theoretical calculations nor in any of the other experimental measurements are the following three sharp structures detected in the present measurement found.

Firstly, the strong peak with a FWHM of about 60 ± 20 meV at 10.04 ± 0.02 eV is caused by the decay of the $^2\Sigma^+$ ($v = 0$) Feshbach resonance at 10.04 eV. No structure is found at 10.305 eV, the postulated energy position of the vibrational $v = 1$ excited level of this resonance. Secondly, a sharp shoulder at 10.41 ± 0.02 eV is visible in the integrated cross section, which can be attributed to the opening of the b $^3\Sigma^+$ ($v = 0$) channel at 10.399 eV. The decay of this state into the A $^1\Pi$ state is forbidden by spin selection rules. The third structure at 10.76 ± 0.02 eV is correlated to the opening of the B $^1\Sigma^+$ ($v = 0$) channel at 10.777 eV, which can decay into the A $^1\Pi$ state by photon emission.

4.4. The d $^3\Delta$ state

In the present study we have measured the energy dependences of the vibrational $v = 20$, 21 and 22 levels of the d $^3\Delta$ state with the excitation energies 9.911, 10.006 and 10.098 eV (values taken from Daviel *et al* 1982), because of their vicinity to the energy position of the $^2\Sigma^+$ Feshbach resonance at 10.04 eV.

To our knowledge only three further experimental groups have measured excitation functions of the peaks located in the energy loss spectrum around 10.0 eV, these are Mazeau and co-workers (1972), Swanson and co-workers (1975) and Allan (1989). In contrast to

us, these groups have attributed the peaks to higher vibrational levels of the a′ $^3\Sigma^+$ state.

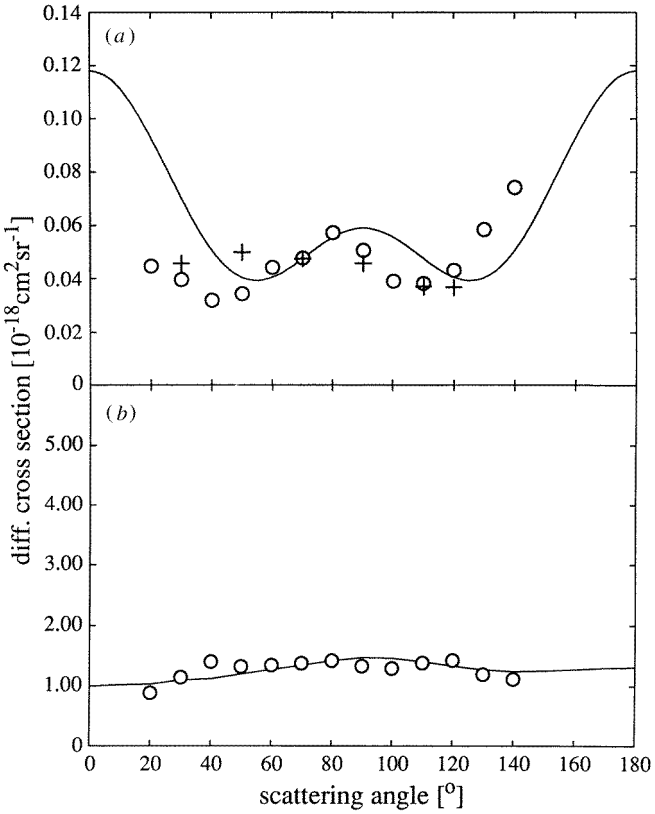

Figure 13. Angular dependence of the X $^1\Sigma^+$ ($v = 0$) → d $^3\Delta$ ($v = 20$) state. (*a*) At the energy position of the $^2\Sigma$ Feshbach resonance (10.04 eV). ○, present result; +, Mazeau *et al* (1972); ——, angular dependence of a dδ partial wave. Both data sets are normalized at 70° to the present result. (*b*) ○, present result at a detection energy $E_d = 3.7$ eV multiplied by a factor of 11 for good visual comparison with the theoretical results (——) of Sun *et al* (1992) at $E_d = 3.5$ eV.

In our measured constant residual energy spectra above 9.6 eV we only found structures caused by vibrational levels of the d $^3\Delta$ state, but no hints for transitions to vibrational levels of the a′ $^3\Sigma^+$ state. Arrow 1 in figure 4 indicates the energy position (9.611 eV) of the $v = 17$ level of the d $^3\Delta$ state. The neighbouring vibrational levels $v = 22$ and 23 of the a′ $^3\Sigma^+$ state are separated more than 25 meV and could therefore be observed as well separated peaks in our experiment, but no structures are visible in the spectrum. Mazeau and co-workers (1972) have measured excitation functions in arbitrary units for a transition with an excitation energy of 9.98 eV at 50°, 90° and 110°. Although they found the onset of the excitation functions to be below the expected threshold at about 9.91 ± 0.03 eV they attributed the measurements to the $v = 26$ level of the a′ $^3\Sigma^+$ state. Assuming here the excitation of the d $^3\Delta$ ($v = 20$) state (excitation energy 9.911 eV), this would explain the detected signal below 9.98 eV. The angular behaviour of the differential cross section of the X $^1\Sigma^+$ ($v = 0$) → d $^3\Delta$ ($v = 20$) transition as well as of the higher vibrational levels $v = 21$ and 22 is found to be rather flat at all detected energies. At each angle the differential cross section starts with a sharp peak close to threshold (caused by the $^2\Sigma^+$ Feshbach resonance

at 10.04 eV) followed by a smooth rise. In figure 13(*a*) we have compared the angular dependence of this peak in the cross section of the d $^3\Delta$ ($v = 20$) state with the results found by Mazeau *et al* (1972) and the angular behaviour of a dδ-partial wave. These two curves are normalized to our absolute value at 70°. The angular behaviour of the peak intensity determined by Mazeau *et al* (1972) agrees quite well with our results. Similar to the behaviour of the dδ partial wave we also find a structure with two neighbouring minima. However, the minima are much less pronounced and are observed at about 15° smaller angles than in the calculated curve, leading to an asymmetry around 90°. This shift may be caused by an interference with the non-resonant part of the scattering amplitude. The excitation mechanism of the d $^3\Delta$ ($v = 20$) state via the $^2\Sigma^+$ Feshbach resonance can be described as

$$\mathrm{X}\ ^1\Sigma^+\ (v = 0, \Lambda = 0) + \mathrm{e}^-(l_{\min} = 0, \lambda = 0) \rightarrow\ ^2\Sigma^+(\Lambda = 0)$$
$$\rightarrow \mathrm{d}\ ^3\Delta\ (v = 20, \Lambda = 2) + \mathrm{e}^-(l_{\min} = 2, \lambda = 2)$$

where Λ, λ and $l_{\min}$ are defined as above. The lowest outgoing $l\lambda$ partial wave for this process has to be a dδ partial wave in agreement with the experiment. In figure 13(*b*) the angular dependence of the d $^3\Delta$ ($v = 20$) state at a detection energy of 3.7 eV is multiplied by a factor of 11 for comparison with the results of Sun *et al* (1992) calculated for nearly the same detection energy (3.5 eV). Both curves show a relative flat distribution over the angular range. The strong rise to lower as well as to higher scattering angles, significant for the excitation of the a′ $^3\Sigma^+$ state (see also figure 10(*c*)), is missing.

Figure 14 compares the integrated cross section of the d $^3\Delta$ ($v = 20$) state with the calculations of Sun *et al* (1992) and of Morgan and Tennyson (1993). Also indicated are

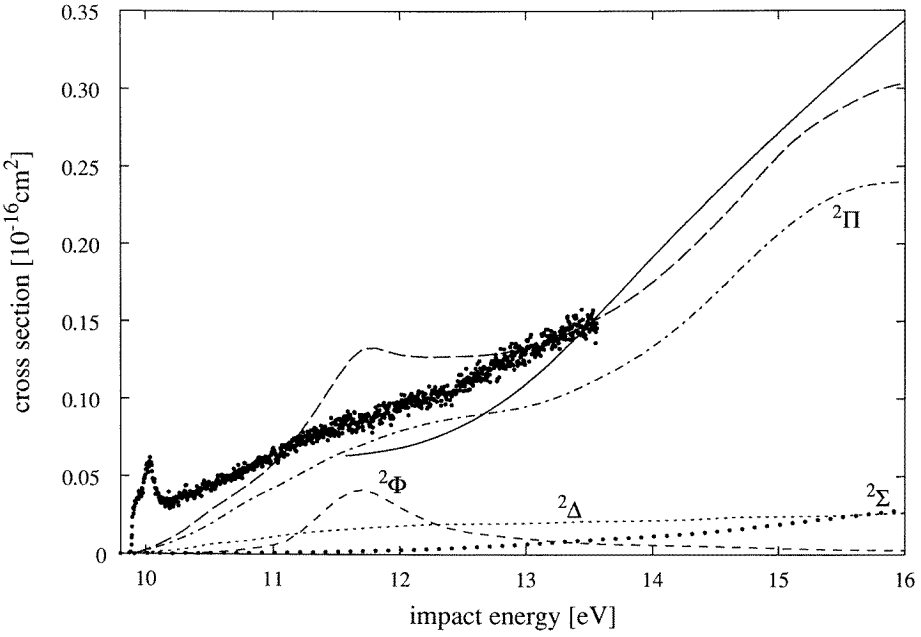

Figure 14. Energy dependence of the cross section of the X $^1\Sigma^+$ ($v = 0$) → d $^3\Delta$ ($v = 20$) transition. ● , present result, multiplied by a factor of 9. Vibrationally summed calculations: ——, Sun *et al* (1992); — — —, Morgan and Tennyson (1993) with resonant contribution (— · —) $^2\Pi$, (· · · · · ·) $^2\Sigma$, (- - - -) $^2\Delta$ and (– – –) $^2\Phi$.

the resonant $^2\Pi$, $^2\Delta$, $^2\Sigma$ and $^2\Phi$ contributions to the cross section calculated by the latter authors. The theoretical curves are shifted to the experimental threshold of 9.911 eV. A broad peak at about 1.6 eV above the threshold caused primarily by the $^2\Phi$ contribution is found in the calculation of Morgan and Tennyson (1993). The calculation of Sun *et al* (1992) and also the experimental integrated cross section do not show a structure at the predicted energy position. Therefore one can conclude that this hypothetical resonance does not have the influence postulated by the calculation of Morgan and Tennyson (1993).

5. Conclusion

We have measured absolute differential cross sections of the spin-forbidden transitions from the X $^1\Sigma^+$ ground state of CO to the valence states a $^3\Pi$, a′ $^3\Sigma^+$ and d $^3\Delta$ and the optically-allowed transition to the A $^1\Pi$ state from threshold to a detection energy of 3.7 eV and from 20° to 140°.

Calculations of the electronic excitation of valence states of CO have predicted six new core-excited shape resonances. Clear evidence for three of these negative ion states with the symmetries $^2\Delta$, $^2\Sigma$ and $^2\Pi$ is found in the experiment. The electron configuration of the $^2\Delta$ and $^2\Sigma$ resonances with the parent a $^3\Pi$ state was determined to be $kl\ 1\pi^4 5\sigma^1 2\pi^2$, while the $^2\Pi$ resonance with the parent a′ $^3\Sigma^+$ state has the electron configuration $kl\ 1\pi^3 5\sigma^2 2\pi^2$. All three resonances are located more than 1 eV above their parent states.

Just at threshold the excitation functions of the a $^3\Pi$ and a′ $^3\Sigma^+$ states start with a steep rise. The measured angular distributions in the threshold region support the assumption of a multichannel resonant decay via the far wing of the $^2\Pi$ resonance located at 1.8 eV. Therefore, the main part of the cross sections of the a $^3\Pi$ and a′ $^3\Sigma^+$ states in the measured energy range are found to be caused by the decay of shape and core-excited shape resonances. This defines an excitation mechanism for the singlet $\rightarrow$ triplet spin-forbidden transitions, where the incoming electron is captured in a resonant state of defined electron configuration, which will decay after a lifetime of about 10^{-15} s by ejecting an electron with an antiparallel spin to that of the incident electron.

In contrast to this, the excitation of the optically allowed transition from the ground state to the A $^1\Pi$ state was found to start at threshold with a value of zero. For this state no dominating resonant partial wave was found in the measured energy range.

The peaks at 9.91, 10.01 and 10.10 eV incident energies in the energy loss spectra of CO could be identified to be the vibrational levels $v = 20$, 21 and 22 of the d $^3\Delta$ state. Except for the structures at the thresholds in the excitation functions of these vibrational levels caused by the $^2\Sigma^+$ (10.04 eV) Feshbach resonance, no further resonant structure has been found in the cross section.

Acknowledgment

The authors gratefully acknowledge the financial support of the Deutsche Forschungsgemeinschaft.

References

Ajello L M 1971 *J. Chem. Phys.* **55** 3158
Allan M 1989 *J. Electron Spectosc. Relat. Phenom.* **48** 219
Borst W L 1971 *Phys. Rev.* A **3** 979
Brongersma H H, Boerboom A J H and Kistemaker J 1969 *Physica* **44** 449
Chang E S 1977 *J. Phys. B: At. Mol. Phys.* **17** L677

Chantranupong L, Bhanuprakash K, Honigmann M, Hirsch G and Buenker R J 1992 *Chem. Phys.* **161** 351
Chung S and Lin C L 1974 *Phys. Rev.* A **9** 1954
Cooper D and Kirby K 1987 *J. Chem. Phys.* **87** 424
Daviel S, Wallbank B, Comer J, Hicks P 1982 *J. Phys. B: At. Mol. Phys.* **15** 1929
Drabbels M, Meerts W L and ter Meulen J J 1993 *J. Chem. Phys.* **99** 2352
Ehrhardt H and Frost L 1993 *Comment. At. Mol. Phys.* **3** 123
Ehrhardt H, Langhans L, Linder F and Taylor H S 1968 *Phys. Rev.* **173** 222
Fisher N J and Dalby F W 1976 *Can. J. Phys.* **54** 258
Fon W C, Lim K P and Sawey P M J 1993 *J. Phys. B: At. Mol. Opt. Phys.* **26** 305
Fournier-Lagarde P, Mazeau J and Huetz A 1984 *J. Phys. B: At. Mol. Phys.* **17** L591
Greene C H and Rau A R P 1982 *Phys. Rev. Lett.* **48** 533
——1983 *J. Phys. B: At. Mol. Phys.* **16** 99
Hammond P, King G C, Jureta J and Read F 1985 *J. Phys. B: At. Mol. Phys.* **18** 2057
Hall R I, Cadez I, Schermann C and Tronc M 1977 *Phys. Rev.* A **15** 599
Halman M and Laulicht I 1965 *Astron. Phys. J. (Suppl.)* **12** 307
Hawley-Jones T J, Read F H, Cvejanovic S, Hammond P and King G C 1992 *J. Phys. B: At. Mol. Opt. Phys.* **25** 2393
Hemminger J C, Cavanagh R, Lisy J M and Klemperer W 1977 *J. Chem. Phys.* **67** 4952
Huber K P and Herzberg G 1979 *Molecular Spectra and Molecular Structure* vol 4 (New York: Van Nostrand Reinhold)
Huetz A, Cadez I, Grestau F, Hall R I, Vichon D and Mazeau J 1980 *Phys. Rev.* A **21** 622
Huo W M 1966 *J. Chem. Phys.* **45** 1554
Joachain C J 1975 *Quantum Collision Theory* vol 1 (Amsterdam: North-Holland) ch 4.5
Jones T S, Ashton M R, Ding M O and Richardson N V 1989 *Chem. Phys. Let.* **161** 467
Kirby-Docken K 1977 *J. Chem. Phys.* **66** 4309
Klar H and Schlecht W 1976 *J. Phys. B: At. Mol. Phys.* **8** 1699
Kopelman R and Klemperer W 1962 *J. Chem. Phys.* **36** 1693
Krupenie P H 1966 *National Standard Reference Data Series* **5**
Kuppermann A, Flicker W M and Mosher O A 1979 *Chem. Rev.* **79** 77
Land J E 1978 *J. Appl. Phys.* **49** 5716
Massey H S W, Burhop E H S and Gilbody H B 1969 *Electronic and Ionic Impact Phenomena* vol II (Oxford: Clarendon)
McKoy V, Winstead C and Pritchard H 1994 Private communication
Mazeau J, Gresteau F, Hall R I, Joyez G and Reinhardt J 1973 *J. Phys. B: At. Mol. Phys.* **6** 862
Mazeau J, Gresteau F, Joyez G, Reinhardt J and Hall R I 1972 *J. Phys. B: At. Mol. Phys.* **5** 1890
Morgan L A and Tennyson J 1993 *J. Phys. B: At. Mol. Opt. Phys.* **26** 2429
Mumma M J, Stone E J and Zipf E C 1971 *J. Chem. Phys.* **54** 2627
Nesbet R K 1979 *Phys. Rev.* A **20** 58
Newman D S, Zubek M and King G C 1983 *J. Phys. B: At. Mol. Phys.* **16** 2247
Pearson P K and Lefebvre-Brion H 1976 *Phys. Rev.* A **13** 2106
Peterkop R K 1971 *J. Phys. B: At. Mol. Phys.* **4** 513
Pichou F, Huetz A, Joyez G and Landau M 1978 *J. Phys. B: At. Mol. Phys.* **11** 3683
Rau A R P 1971 *Phys. Rev.* A **4** 207
Read F H 1968 *J. Phys. B, Proc. Phys. Soc. Ser.* 2 **1** 893
——1984 *J. Phys. B: At. Mol. Phys.* **17** 3965
——1985 *Electron Impact Ionization* ed G H Dunn and T D Mark (New York: Springer) p 42
Rosenkrantz M E and Kirby K 1989 *J. Chem. Phys.* **90** 652
Schubert E, Jung K and Ehrhardt H 1981 *J. Phys. B: At. Mol. Phys.* **14** 3267
Selles P, Huetz A and Mazeau J 1987 *J. Phys. B: At. Mol. Phys.* **20** 5195
Skubenich V V 1967 *Opt. Spektrosk.* **23** 990
Srivastava S K, Chutjian A and Trajmar S 1975 *J. Chem. Phys.* **63** 2659
Sun Q, Winstead C and McKoy V 1992 *Phys. Rev.* A **46** 6987
Swanson N, Celotta R J, Kuyatt C E and Cooper J W 1975 *J. Chem. Phys.* **62** 4880
Teillet-Billy D, Malegat L and Gauyacq J P 1989 *J. Phys. B: At. Mol. Opt. Phys.* 22 1095
Teillet-Billy D, Malegat L, Gauyacq J P, Abouaf R and Benoit C 1987 *J. Phys. B: At. Mol. Phys.* **20** 3201
Tilford S G and Simmons J D 1972 *J. Phys. Chem. Data* **1** 147
Trajmar S, Williams W and Cartwright C 1971 *Proc. 7th Conf. on Physics of Electronic and Atomic Collisions* (Amsterdam: North-Holland) Abstracts p 1066

Trajmar S, Williams W and Cartwright C 1973 *Proc. 8th Conf. Physics of Electronic and Atomic Collisions* (Zrenjanin: Grafico Preduzece 'Buducnost') p 349
Trajmar S 1994 Private communication
Wallbank B, Daviel S, Comer J and Hicks P 1983 *J. Phys. B: At. Mol. Phys.* **16** 3065
Wannier G H 1953 *Phys. Rev.* **90** 817
Weatherford C A and Huo W M 1990 *Phys. Rev.* A **41** 186
Wicke B G, Field R W and Klemperer W 1972 *J. Chem. Phys.* **56** 5758
Wicke B G and Klemperer W 1975 *J. Chem. Phys.* **63** 3756
Wigner E P 1948 *Phys. Rev.* **73** 1002
Wolk G L and Rich J W 1983 *J. Chem. Phys.* **79** 12
Wong S F and Schulz G J 1974 *Phys. Rev. Lett.* **33** 134